Decentralized algorithms for consensus-based power packet distribution

AUTHOR(S):

Baek, Seongcheol; Ando, Hiroyasu; Hikihara, Takashi

NOLTA, IEICE

Paper

Decentralized algorithms for consensus-based power packet distribution

Seongcheol Baek [1 a)], *Hiroyasu Ando* [2,3 b)], *and Takashi Hikihara* [1 c)]

[1] *Department of Electrical Engineering, Kyoto University*
Katsura, Nishikyo, Kyoto 615-8510, Japan

[2] *Faculty of Engineering, Information and Systems, University of Tsukuba*
1-1-1 Tennodai, Tsukuba 305-8573, Japan

[3] *Advanced Institute for Materials Research, Tohoku University*
2-1-1 Katahira, Aoba-ku, Sendai 980-8577, Japan

[a)] *s-baek@dove.kuee.kyoto-u.ac.jp*
[b)] *ando@sk.tsukuba.ac.jp*
[c)] *hikihara.takashi.2n@kyoto-u.ac.jp*

Received October 29, 2020; Revised December 7, 2020; Published April 1, 2021

Abstract: Power packets are proposed as a transmission unit that can deliver power and information simultaneously. They are transferred using the store-and-forward method of power routers. A system that achieves power supply/demand in this manner is called a power packet network (PPN). A PPN is expected to enhance structural robustness and operational reliability in an energy storage system (ESS) with recent diverse distributed sources. However, this technology is still in its early stage and faces numerous challenges, such as high cost of implementation and complicated energy management. In this paper, we propose a novel power control based on decentralized algorithms for a PPN. Specifically, the power supply is triggered and managed by communications between power routers. We also discuss the mechanism of the decentralized algorithm for the operation of power packets and reveal the feasibility of the given control method and application by forming biased power flows on the consensus-based distribution.

Key Words: power packet, complex communication, decentralized algorithm, consensus dynamics, communication network, energy management, network design, network dynamics

1. Introduction

With the recent emergence of distributed power sources and the shifting trend from fuel engines to electrical motors along with the advancement of battery efficiency, the decentralization technique has attracted considerable attention from the fields of mechanical, control, and network engineering. The characteristics of the next-generation power system, such as high fluctuations, in-demand generation,

Nonlinear Theory and Its Applications, IEICE, vol. 12, no. 2, pp. 181–193 DOI: 10.1587/nolta.12.181

and combined use of batteries and other power sources, have resulted in the consideration of more delicate controls by system engineers. In a smart grid, for example, load peak shaving and power smoothing are the common methods that are considered [1, 2]. From the viewpoint of system design, decentralization can be sufficiently applied to achieve scalability and flexibility, thanks to the system operation based on the agent-to-agent communication and interaction [3].

A power packet network (PPN) is motivated by an initial concept of open electric energy network (OEEN) which is introduced to enable power trading between participants, such as in the energy industry in the USA [4]. Although the scale of distribution and the expected applications are different from its origin, a PPN employs a key concept: the introduction of a communication system to power system [5]. Specifically, in a PPN, the power routers generate power packets with pulsed power sequences, and the semantic functions are granted by dividing the bit strings in the unit power packet into informational tag and power payload [5, 6]. Power packet transmissions between routers are performed using the store-and-forward method [7, 8]. This method relaxes the strict balancing rule of supply/demand and provides network buffer to shift power flow temporally and spatially. Thus, a PPN is expected to exhibit high controllability in energy management as well as adaptivity to deal with diverse energy conditions.

Recent studies on PPN cover a variety of spectra, such as dynamics, devices, control theory, energy storage system, and applications. Nawata *et al.* proposed a symbol-based transmission model that can explain power flow based on a symbol propagation matrix [9]. T. Hikihara *et al.* proposed another theoretical approach which suggested that the flow of power packets can be quantized and developed into the Schrodinger equation [10]. In the related studies to PPN, the research group of E. Gelenbe has proposed a methodology for the implementation, utility, and optimization of the energy packet network through the problem of energy packet distribution on overlapped network of information processing layer and energy processing layer [11, 12]. Moreover, related technical discussions have indicated the application of synchronization to enable a stable exchange of information between routers [13], as well as a security strategy with the use of power packets [14]. In relation to our previous works, H. Ando *et al.* proposed the consensus dynamics to analyze the dynamics of the power packet transmission and to capture characteristics originating from the connections on the network [15, 16]. Moreover, we further discussed the relationship between the above model and the emulation initiated by the decentralized control of a PPN [17, 18]. This work provides a theoretical understanding of the consensus-based packet distribution and the possibility of the decentralized control of a PPN.

With the recent advancements of distributed power sources, scalability and flexibility have become important characteristics in the network design and its application. A potential vision of a PPN has been proposed through the operation of motors and load control based on power packets [19, 20]. However, a system with different purposes and structures used in the semantic/schematic design is costly. Based on this context, a decentralized algorithm-based control that is independent of the topological structure of a PPN is proposed, thus eventually improving scalability, flexibility, and redundancy. For power packet transmission, we employ the consensus-based distribution model and consider two operational strategies: the top-down (or supply-driven) method and the bottom-up (or demand-driven) method. Moreover, we reveal a feasible application of energy management using both strategies, in which power flows can be prioritized to power routers of the bottom-up method.

The remainder of this paper is organized as follows. Section 2 introduces the PPN. Section 3 discusses the graphical analysis and interpretation of a PPN, and the consensus-based distribution model to capture the dynamics of power flow. Next, we propose a decentralized algorithm for a PPN on the basis of the routers' communication and distribution model. Section 4 explains the packet distribution scenario for two network structures and simulates the decentralized control of a PPN. The results the simulation reveal the feasibility of the proposed control methods and the possibility for a priority-based power control using the top-down and bottom-up methods. Finally, Section 5 concludes the paper.

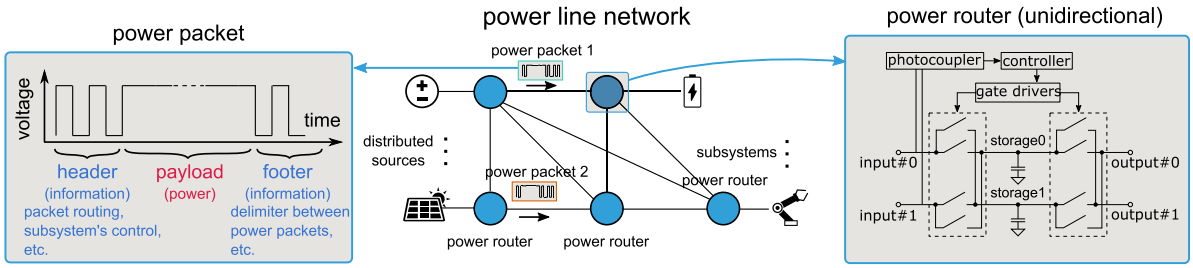

Fig. 1. Layout of a power packet network (PPN). Using the store-and-forward method, the power routers deliver the power packets from the supply side to the demand side.

2. Power packet network

In Fig. 1, the schematic diagram of a PPN is presented. Given the pulsed direct current (DC) power, a power packet consists of bit sequences of information tag and power payload. An information tag denoted as "header" and "footer," delivers information using coded bit sequences. Specifically, information on the routing address or control signal is placed in the "header," and a delimiter is embedded in "footer" to signal the termination of packet transmission. The power payload physically delivers the electric power from the sender to the receiver.

A power router generates or receives the power packets with built-in switches and storages [6]. This allows the group of routers to actively control the power flows on each of the connected ports. Specifically, a power router detects the inflow of power packets through a photocoupler. The incoming header information is processed in the controller and delivered to the gate driver to control each of the built-in switches, thus opening the corresponding port to charge built-in storages with power inflow (payload). Subsequently, if the footer is detected, the online port is closed, and the transmission of the given power packet is terminated. In addition to storing power packets, a power router can also forward power packets by generating pulses with switches and charged storage. The use of the store-and-forward method results in the quantization of power flows and simultaneous transmission of both power and information.

With the implementation of power routers, a PPN can accommodate multilevel DC sources and deliver power packets to the demanding subsystem. Since power packets contain routing information and optionally control information, the transmission network can handle several loads (subsystems) with shared lines, which is called time-division multiplexing. In terms of the recent progress of distributed power sources, the integrity and flexibility of PPN are expected to solve the emerging issues on power management, such as energy security, sporadic growth of grid, large loss due to oversupply, and unpredictability of renewable energy [21].

The structure of a PPN lies in its switching topology, which is a notable feature. Specifically, the paths where power packets go through are not constant. Each path gets connected or disconnected, depending on the routers' operation [22]. Another feature of a PPN is that the power packet transmission is controlled autonomously by routers, which is thanks to the high-speed field-programmable gate array platform [23]. In addition, the autonomous operation on each power router leads to the possibility of a decentralized control system (DCS) on PPN. A DCS improves the reliability in both energy management and failure management, as well as structural scalability that is a challenge in the previous power system.

3. Modeling of decentralized algorithm for a power packet network

Provided that a system is driven in a decentralized manner, the spread dynamics of physical quantity or information can be explained based on the agent-to-agent interaction. Given this idea, we employ the consensus dynamics to elucidate the distribution of power flows on a PPN and model a decentralized algorithm.

3.1 Outline of the graphical analysis of a power packet network

For simplicity, we assume that each of the routers is bidirectional and has a single storage or DC

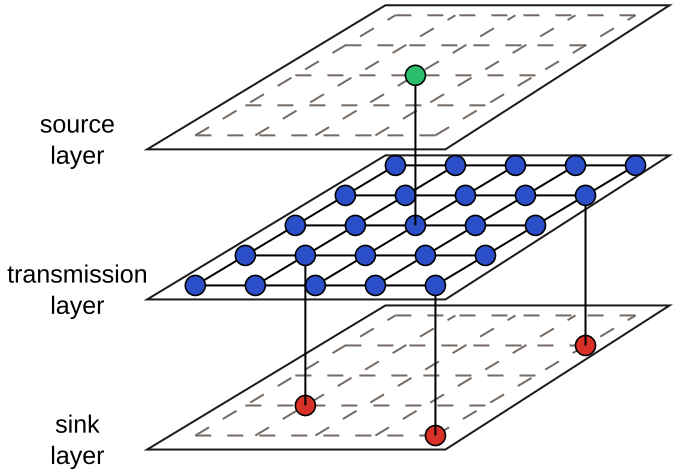

Fig. 2. A three-layered schematic of a PPN. The nodes in the source layer, transmission layer, and sink layer indicate the power routers with a source, power routers with a storage, and GNDs, respectively. The on-resistances of the routers' switching devices and loads are located on each path. The power flows through the source layer and is distributed to the transmission layer; it then flows out through the sink layer.

source. Given a transmission network, such as in Fig. 1, we consider a graph notation $G(\boldsymbol{V}, \boldsymbol{E}, \boldsymbol{c}, \boldsymbol{w})$, with $\boldsymbol{V}$ denoting the nodes; $\boldsymbol{E}$, the edges; $\boldsymbol{c}$, the node weight; and $\boldsymbol{w}$, the edge weight. The nodes represent a set of power sources, a storage in routers, and outflow sinks (GNDs). The edges are given as transmission paths, including the ideal line resistance. The generalized impedance can also be considered in the analysis of the algebraic graph [24, 25]. Thus, any edge between two connected nodes involves the line resistance r, of which reverse is given as edge weight w, *i.e.*, $w_{ij} = r_{ij}^{-1}$ for path e_{ij}. The node weights are given as capacitances of nodes indicating that the storage capacitance c_i is directly applied as a node weight of node u_i. In case of sources and sinks, we assume that the node weight is positive infinity.

Figure 2 presents a multilayered schematic network of $G(\boldsymbol{V}, \boldsymbol{E}, \boldsymbol{w}, \boldsymbol{c})$ based on the divided three node groups. The divided layers facilitate the visualization of power flows between sources and sinks. From the given schematic, the node voltage vector on the source layer is denoted as $\boldsymbol{v}_{\mathrm{src}}$, the node voltage vector on the transmission layer as $\boldsymbol{v}$, and the rest on the sink layer as $\boldsymbol{v}_{\mathrm{snk}}$. Here, $\boldsymbol{v}_{\mathrm{src}}$ denotes a positive constant vector, and $\boldsymbol{v}_{\mathrm{snk}}$ denotes a zero constant vector.

$$\boldsymbol{v}_{\mathrm{src}} = \mathrm{const.} > 0 \tag{1}$$

$$\boldsymbol{v}_{\mathrm{snk}} = 0 \tag{2}$$

Each of the paths between the nodes has a weight; if path e_{ij} is switchable, its weight is defined as $\{0, r_{ij}^{-1}\}$, depending on its switching state. If the path is routed, the weight is given as r_{ij}^{-1}; otherwise, 0. This is reasonable because if the path is disconnected, the line resistance is obtained as ∞, of which reverse is 0.

For a multilayered network, the spread dynamics of matters or information is considered. The consensus dynamics provides a useful analysis for problems, such as collective behavior of flocks and swarms, formation control for multirobot systems, synchronization of coupled oscillators, consensus-based belief propagation, and so on [22, 26, 27]. Given a variable $x_{i\in\{0,\cdots,n-1\}}$ for each node on graph G, the spread process is described as follows in terms of node u_i:

$$c_i \dot{x}_i = \sum_{j\in\{k;(i,k)\in E(G)\}} w_{ij}(x_j - x_i) + b_i, \tag{3}$$

where c_i indicates the node weight; w_{ij}, the edge weight; and b_i, bias. Here, we assume a general variable x_i, such as matters or information in the system. The above equation is generalized using the weighted Laplacian (or edge-weight Laplacian matrix) $\boldsymbol{L}(G)$ and a node-weight matrix $\boldsymbol{C} = \mathrm{diag}(c_0, \cdots, c_{n-1})$ [22].

$$\boldsymbol{C}\dot{\boldsymbol{x}} = -\boldsymbol{L}\boldsymbol{x} + \boldsymbol{b} \tag{4}$$

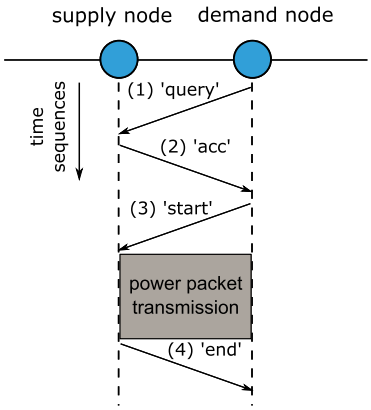

Fig. 3. A communication logic of the bottom-up method between two power routers. In the bottom-up method, the power packet transmission is triggered by the demand-side node; thus, the communication sequence is started with the "query" message from the demand-side node. Conversely, in the top-down method, the power packet transmission is triggered by the supply-side node, which results in the omission of the "query" message and the sequence being started with the 'acc' message from the supply-side node.

Following this, the relation based on a discrete time is obtained as follows.

$$\boldsymbol{x}(k+1) = (\boldsymbol{I} - \epsilon \boldsymbol{C}^{-1}\boldsymbol{L})\boldsymbol{x}(k) + \epsilon \boldsymbol{C}^{-1}\boldsymbol{b} \tag{5}$$

The state-transition matrix, which is expressed as $(\boldsymbol{I} - \epsilon \boldsymbol{C}^{-1}\boldsymbol{L})$ in Eq. (5), is stable in the case of connected graph G and $0 < \epsilon < 1/\max_{i\in V}(c_i^{-1}\sum_j w_{ij})$; thus, with condition $\boldsymbol{b} = \boldsymbol{0}$, each element of $\boldsymbol{x}$ asymptotically reaches a weighted average. The consensus dynamics further provides an estimation for the spread performance, which is often based on algebraic connectivity $\lambda_2(\boldsymbol{L})$ or eigendecomposition [22, 26].

3.2 Power dynamics of the consensus-based distribution

On a PPN, such as in Fig. 2, the occurrence of power packet transmissions can be assumed, causing the power flows from the source layer to sink. Let us consider a node voltage $\boldsymbol{v}$ for the variable $\boldsymbol{x}$ in Eq. (4). Considering that $\boldsymbol{b} = 0$ and the left term in Eq. (4) is the net current of the node, the following relation is derived:

$$\boldsymbol{i}_{\text{net}} = -\boldsymbol{L}\boldsymbol{v} \tag{6}$$

Now it can be easily observed that $\boldsymbol{L}$ denotes the inverse of network resistance, because $\boldsymbol{w} = \{w_{ij}; e_{ij} = (i,j) \in \boldsymbol{E}\}$ is adopted based on the line resistance (or impedance generally). Since the paths switch depending on the routers' operation, the weighted Laplacian is a time-varying variable in terms of time t, which is expressed as $\boldsymbol{L} = \boldsymbol{L}(S_t(G))$ with a subgraph $S_t(G) = G(\boldsymbol{V}, \boldsymbol{E}_t)$, where $\boldsymbol{E}_t \subset \boldsymbol{E}$. From the three-layered model presented in Fig. 2, Eq. (6) is further improved with current inflow $\boldsymbol{i}_{\text{in}}$ and outflow $\boldsymbol{i}_{\text{out}}$.

$$\begin{bmatrix} \boldsymbol{i}_{\text{in}} \\ \boldsymbol{C}\dot{\boldsymbol{v}} \\ \boldsymbol{i}_{\text{out}} \end{bmatrix} = - \begin{bmatrix} \boldsymbol{L}_{11} & \boldsymbol{L}_{12} & \boldsymbol{L}_{13} \\ \boldsymbol{L}_{21} & \boldsymbol{L}_{22} & \boldsymbol{L}_{23} \\ \boldsymbol{L}_{31} & \boldsymbol{L}_{32} & \boldsymbol{L}_{33} \end{bmatrix} \begin{bmatrix} \boldsymbol{v}_{\text{src}} \\ \boldsymbol{v} \\ \boldsymbol{v}_{\text{snk}} \end{bmatrix}, \tag{7}$$

Note that each element $\boldsymbol{L}_{ij}$ of the weighted Laplacian is time-varying. Assuming the constant voltages in the source and sink layers, *i.e.*, $\boldsymbol{v}_{\text{src}} = \text{const.}$ and $\boldsymbol{v}_{\text{snk}} = \boldsymbol{0}$, the following dynamics can be obtained, which explains the voltage distribution on a PPN.

$$\dot{\boldsymbol{v}} = -\boldsymbol{C}^{-1}\boldsymbol{L}_{22}\boldsymbol{v} - \boldsymbol{C}^{-1}\boldsymbol{L}_{21}\boldsymbol{v}_{\text{src}} \tag{8}$$

3.3 Modeling of decentralized algorithms

Figure 3 presents the communication sequences between two adjacent nodes for power packet transmission. To accomplish the power packet transmissions, the communication sequences consist of four messages; "query," "acc," "start," and "end," which refer to "packet-request," "transmission-available,"

"transmission-start," and "transmission-end," respectively. First, if a node satisfies $g_i(t) \geq 0$ given in Eq. (9), it sends a "query" signal to the adjacent nodes. Then, the "acc" message is returned if the adjacent node j satisfies the condition $g_j(t) < 0$.

$$g_i(t) = c_i^{-1} w_{ij^*}(v_{j^*} - v_i) \quad \text{s.t.} \quad j^* = \underset{j \in \{k;(i,k)\in E\}}{\arg\max} \; w_{ij}|v_j - v_i| \tag{9}$$

Note that g_i is given as a potential consensus-based distribution model in Eq. (3), and also indicates the maximum absolute value of the voltage difference between node i and the adjacent node j. After receiving the "acc" message, the demanding node sends the "start" message and prepares to receive a power packet. When the "start" message is received, the adjacent node sends a power packet to the target node, which results in a routing $w(e_{ij}) = r_{ij}^{-1}$ between two nodes during single power packet transmission. After the termination of the transmission, the supply node sends the "end" message to the demand node, and the path e_{ij} is unrouted with $w(e_{ij}) = 0$.

Based on the above schematics, a decentralized algorithm is provided in Fig. 4. The algorithm is divided into three loops: "termination of transmission," "forwarding packet," and "storing packet". The decentralized algorithm begins with the "initialize" mode. Then, when a node satisfies a condition $\mathrm{e{\cdot}t} \geq \Delta t_u$ meaning that the duration of the mode exceeds the given value Δt_u, it transitions to the "termination of transmission" loop. In this loop, the node checks whether it has received the "end" message at each port. If the "end" message is received at the specific port, the node terminates the power packet transmission, thus eventually closing the corresponding route. Otherwise, the node holds its routing state. When all ports are checked in the "termination of transmission" loop, the node transitions to the "evaluate" mode, which determines whether it stores or forwards a power packet based on the evaluation function g_i.

In the "storing packet" loop, the node checks whether it has received the "acc" message from each port. If the node has received the "acc" message, it sends back the "start" message and initiates the power packet transmission. Otherwise, the node sends the "query" message to its adjacent nodes. After checking all ports, the node transitions to the "initialize" mode.

In the "forwarding packet" loop, the node checks whether it has received the "query" message at each port. If the node has received the "query" message, it replies the "acc" message and waits for the "start" message. After receiving the "start" message from the adjacent node, the node starts to send a power packet. When a single power packet is completely sent, the node tags the "end" message. After checking all ports, the node transitions to the "initialize" mode.

4. Simulations

Using the decentralized algorithms, two PPN structures are simulated to evaluate the feasibility and features of the proposed control method. It should be noted that the proposed control method is structure-independent, indicating that the applied algorithms are identical, regardless of the network structure.

4.1 Simulation settings

To simulate the power packet transmission, we assume two networks, which are given as a 1D chain structure (Fig. 5(a)) and triangular mesh structure (Fig. 5(b)). In each case, the power packets are generated from the source nodes (indicated in green), delivered through the storage nodes (indicated in blue), and then dissipate at sink nodes (indicated in red). As discussed in Section 3.1, all the impedances, including the switching resistances and loads, are considered in the edge weights, specifically, $w_{ij} = r_{ij}^{-1}$ in the case of the connected path e_{ij}.

Throughout the simulations presented in Fig. 5, the following parameters are commonly assumed. In both cases, the voltage of the source node v_0 is set to 10 V, and the initial voltage of the storage nodes is selected from the random values in $[0, 10]$, following a uniform distribution. The capacitance of each storage node is set to 1000 μF. For the property of the power packet, the bit time is set to 3.125 μs, and the bit length to 100; thus, the duration of the unit power packet becomes $T_p = 312.5\,\mu$s. Moreover, 10 bit of the unit power packet is considered as an abstract information tag. Hence, during

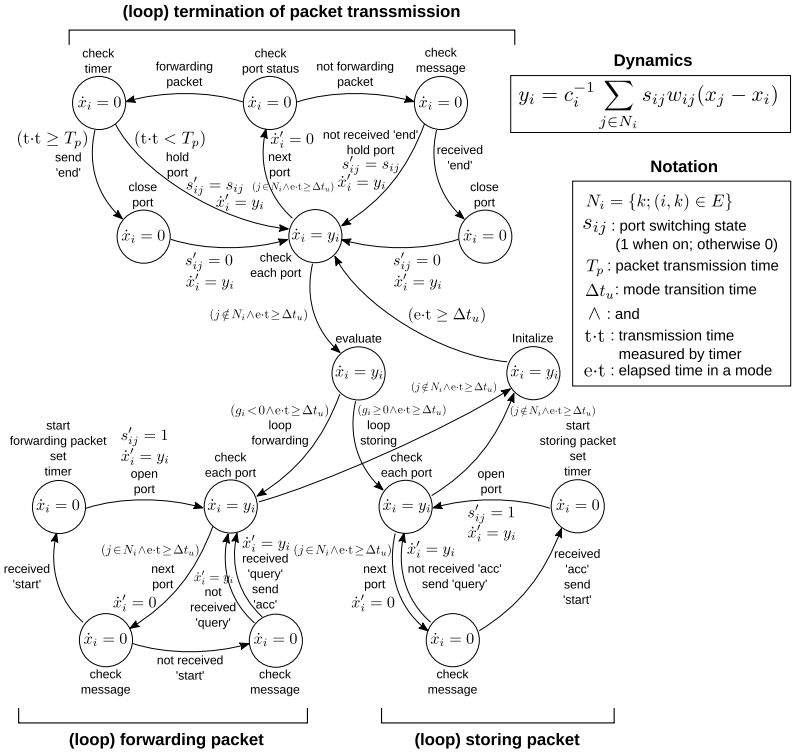

(a)

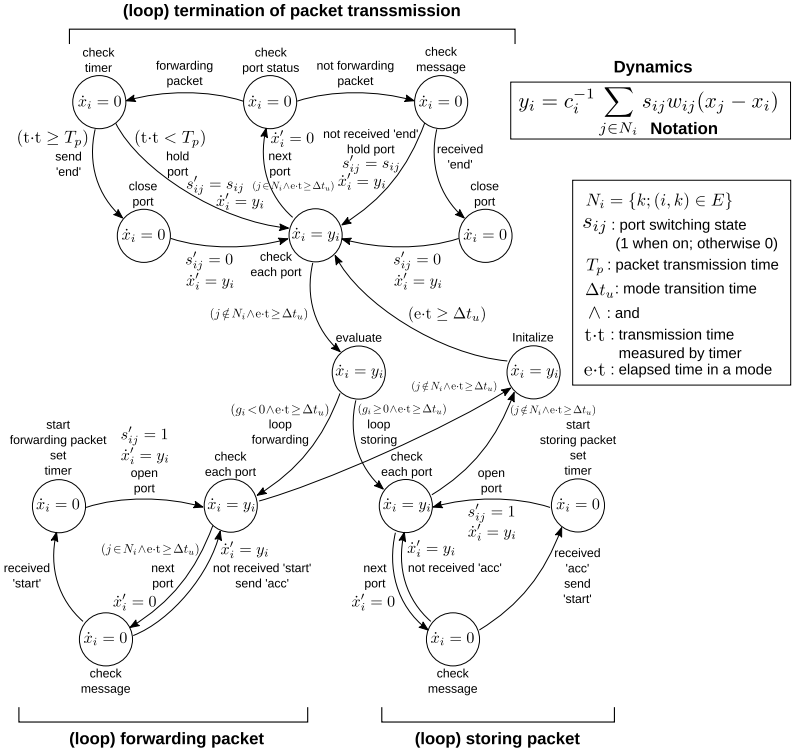

(b)

Fig. 4. Decentralized algorithms of the (a) bottom-up method and (b) top-down method for a power router. The algorithm is divided into three loops: termination of packet transmission, packet forwarding, and packet storing. The bottom-up method and top-down method employ the different loops of packet forwarding and packet storing, according to each of the communication logics. Here, the parentheses () indicate the transition conditions, and the superscript-(′) denotes the updated values when transitioned.

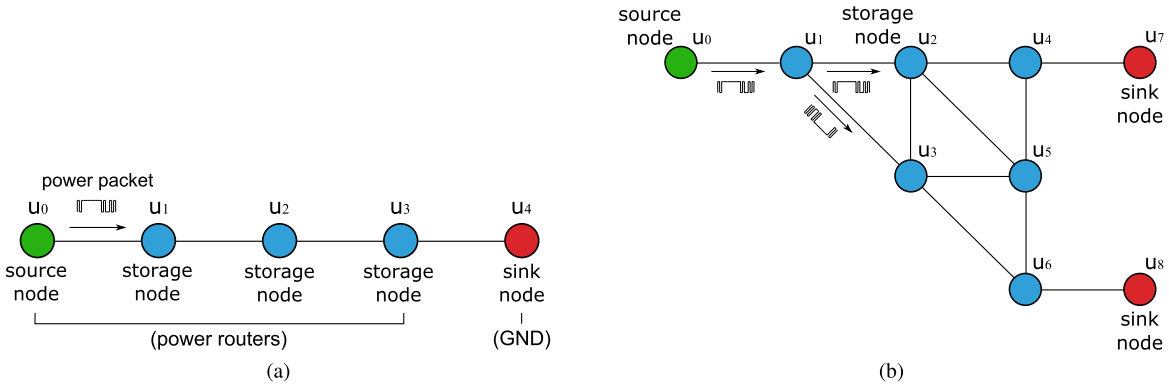

Fig. 5. Topological structures of a PPN of (a) a 1D chain network and (b) a triangular mesh network. The green nodes indicate power routers with source; the blue nodes, power routers with a storage; and the red nodes, sink nodes (GNDs).

the power packet transmission of, power flow is allowed in only 90 % of its duration. For the power routers corresponding to the source nodes and storage nodes, the switching resistance is set to $1\,\Omega$. This leads to $0.5\,\Omega^{-1} = (1\,\Omega + 1\,\Omega)^{-1}$ of the edge weight when connected, because two switching devices are located on the source-to-storage or storage-to-storage paths. In the case of a disconnected condition, the edge weight is set to 0. In addition, we assume $50\,\Omega$ of loads adjacent to sink nodes, which gives a storage-to-sink edge weight of $0.0196\,\Omega^{-1} = (1\,\Omega + 50\,\Omega)^{-1}$. For simplicity, we assume that the paths of the storage node and sink node are connected during the entire simulation. In the applied decentralized algorithms, the mode transition time is set to $\Delta t_u = 10\,\mu$s.

In both the simulations presented in Fig. 5, the bottom-up method and top-down method presented in Fig. 4 are applied. In addition to the simulations presented in Fig. 5(b), a mixed control method is applied to test the difference between the two proposed control methods. Specifically, the top-down method is applied to node u_0, u_1, u_2, and u_4, whereas the bottom-up method is applied to node u_3, u_5, and u_6. Here, each node group to which the two methods are applied is clustered in a connected relationship, and the interaction paths between the two groups are maximized to four; e_{13}, e_{23}, e_{25}, and e_{45}, of which setting is intended to check the noticeable difference in the power flow into u_7 and u_8. The dynamics of power is calculated using Eq. (8). Given these simulation settings, a power packet transmission is simulated 10 times for each control method on each network structure presented in Fig. 5(a) and Fig. 5(b).

4.2 Results

For the given PPN in Fig. 5, power packet transmissions were simulated using the bottom-up, top-down, and mixed control methods. Each simulation recorded the time series for node voltages and path power flows as well as the distribution of voltage and power at the end time of the simulations. For the results of the 1D chain network presented in Fig. 5(a), a simulation case with time series for node voltages and path powers was obtained, as in Fig. 6; each of the endpoints for 10 cases was obtained as in Fig. 7.

From the results presented in Fig. 6(a) and Fig. 6(b), the bottom-up method exhibited more fluctuations than the top-down method. This is because the bottom-up method requires extra communication sequences starting with the "query" message compared with the top-down method. Accordingly, this result indicates that the rate of the power packet transmission using the bottom-up method is slightly low, which resulted in the low voltage distribution in nodes 1, 2, and 3, as presented in Fig. 7(a) in comparison with Fig. 7(b). This also caused higher differences in the voltage distributions among nodes 0, 1, 2, and 3 using the bottom-up method. As a result, larger fluctuations in the path of power flows were observed, as presented in Fig. 6(c) compared with the result of Fig. 6(d). Moreover, in the multiple simulation cases presented in Fig. 7(c) and Fig. 7(d), a variance of formed power throughputs is higher using the bottom-up method compared with the top-down method. These results indicate that the power packet transmission is more sparse in the case of transmission among nodes using the

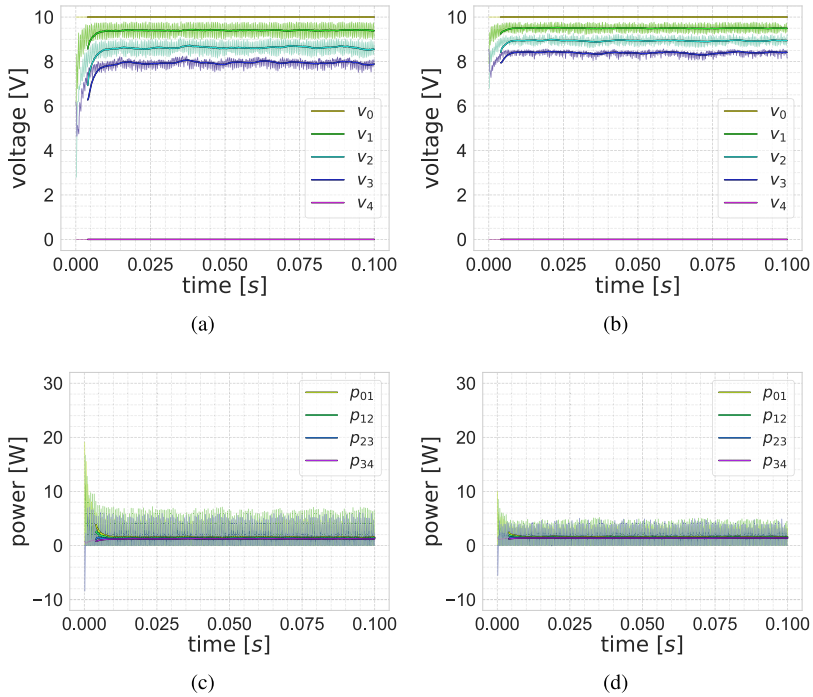

Fig. 6. A simulation case of the time series data of the node voltages and path powers on 1D chain network (Fig. 5(a)). From the top left, each subfigure represents the voltage data of the (a) bottom-up method and (b) top-down method as well as the power data of the (c) bottom-up method and (d) top-down method, respectively. In each simulation, the initial voltage of the storage nodes is selected from the random values in $[0, 10]$. The solid lines indicate the moving average with a window size of 1.25 ms, which is based on the light-colored actual data.

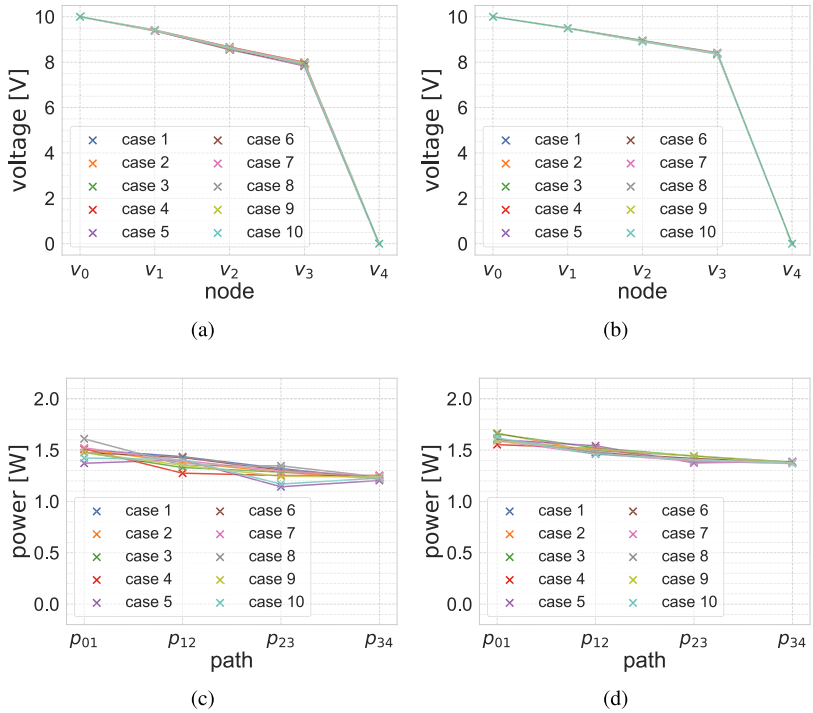

Fig. 7. The voltage distribution and power throughputs of the moving average data on 1D chain network (Fig. 5(a)) at $t = 0.1$ s. From the top left, each subfigure represents the voltage data of the (a) bottom-up method and (b) top-down method, as well as the power data of the (c) bottom-up method and (d) top-down method, respectively.

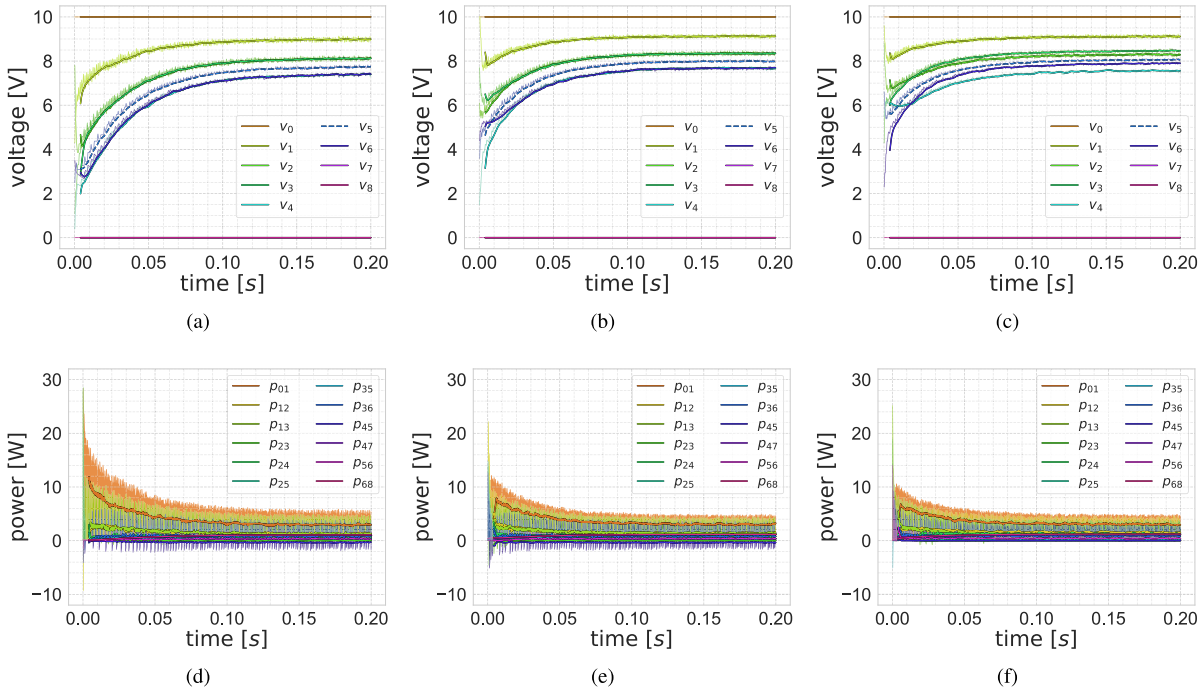

Fig. 8. A simulation case of time series data of node voltages and path powers over time on triangular mesh network (Fig. 5(b)). From the top left, each subfigure represents the voltage data of the (a) bottom-up method, (b) top-down method, and (c) mixed control method as well as the power data of the (d) bottom-up method, (e) top-down method, and (f) mixed control method, respectively. In each simulation, the initial voltage of the storage nodes is selected from the random values in $[0, 10]$. The solid lines indicate the moving average with a window size of 1.25 ms, which is based on the light-colored actual data. Exceptionally, in the figures of node voltage, the dashed line for v_5 is used to clarify the distinction from other solid lines.

bottom-up method compared with that using the top-down method.

From the simulations performed on the 1D chain structure presented in Fig. 5(a), a plain characteristic can be derived, *i.e.*, in the given decentralized control, the top-down method exhibits better performance in power broadcasting. While the top-down method focuses on the supply-driven packet distribution, the bottom-up method deals with the demand-driven packet distribution (also called demand response). In the simulations of the top-down method and the bottom-up method in this paper, all node of PPN is basically assumed to be requesting for power packets. Due to this setting, it is difficult to capture the remarkable difference between the two methods. This problem is explained in the following simulation with the mixed control method.

In the simulation of a triangular mesh network in Fig. 5(b), the time series data and distribution of voltages and powers were obtained in Fig. 8 and Fig. 9, respectively. By comparing the bottom-up case to the top-down case, as presented in Fig. 8(a), Fig. 8(b), Fig. 9(a), and Fig. 9(b), the overall aspect of the voltage distribution was similar to that in the simulation performed on the structure presented in Fig. 5(a). More specifically, the voltage distribution is gradually reduced according to the topological distance to the source node. In addition, the higher path degree of the inflow led to a high voltage status as shown in node v_5 comparing to nodes v_4 and v_6 in the same topological distance to the source node. The overall voltage distribution in the top-down case was higher than that in the bottom-up case. This result agrees with those from the previous results of Fig. 7(a) and Fig. 7(b).

From the results of power flows obtained, as presented in Fig. 8(d), Fig. 8(e), Fig. 9(d), and Fig. 9(e), larger fluctuations were observed in comparison with the simulations performed on the 1D chain structure. If a temporal imbalance or fluctuation exists in the same stage's nodes, resilience is induced by the consensus-based distribution model employed in the decentralized algorithms of each node. Specifically, in the voltage fluctuation shown as in Fig. 8(a) and Fig. 8(b), the voltage distributions of v_4 and v_6 were supposed to be balanced due to the symmetry of the network topology and the same

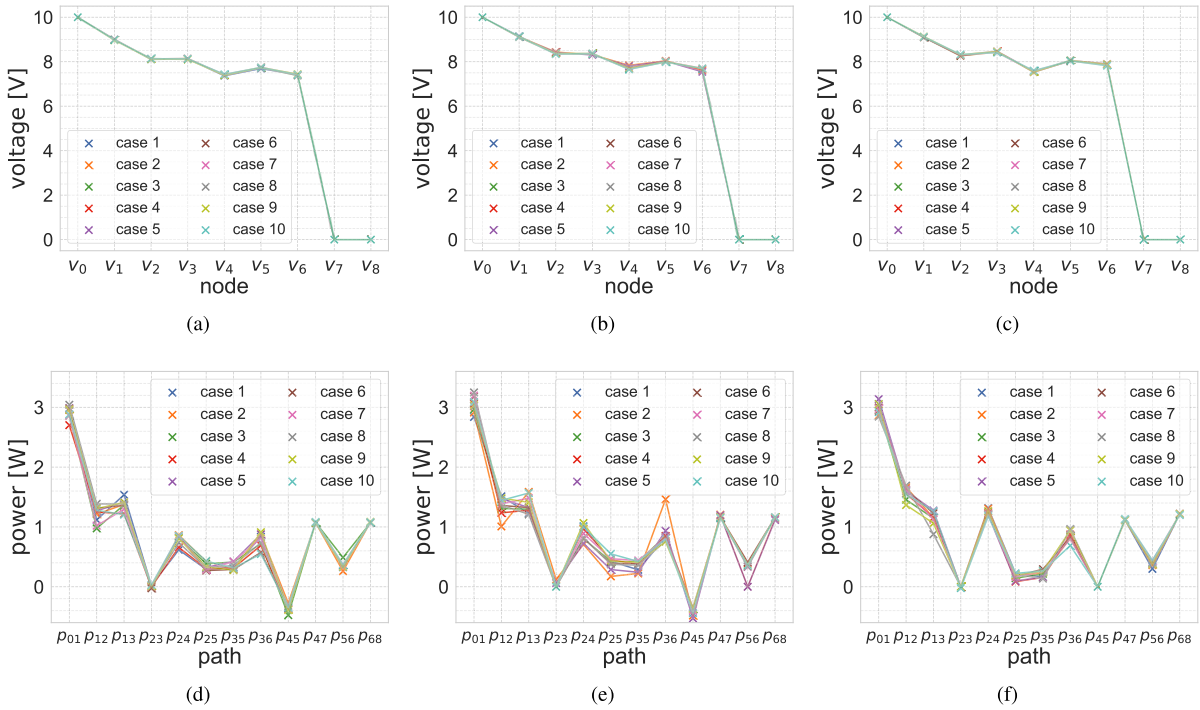

Fig. 9. The voltage distribution and power throughputs of moving average data on triangular mesh network (Fig. 5(b)) at $t = 0.2$ s. From the top left, each subfigure represents the voltage data of the (a) bottom-up method, (b) top-down method, and (c) mixed control method, as well as the power data of the (d) bottom-up method, (e) top-down method, and (f) mixed control method, respectively.

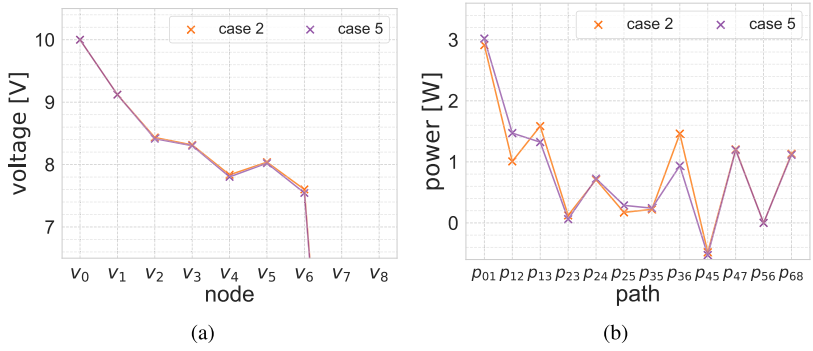

Fig. 10. The results of the case 2 and 5 from Fig. 9(b) and Fig. 9(e). In the (a) voltage distribution, the range of y axis is rearranged to emphasize the difference between nodes 4 and 6, as well as the difference between nodes 2 and 3.

algorithm applied. However, for case 2 and 5 in Fig. 10(a), v_4 was slightly higher than v_6, thus causing a small gap between p_{47} and p_{68}, as presented in Fig. 10(b). These are presumed to be temporary and on the balancing process, seeing that p_{36} is larger than p_{24} at the given period, as well as p_{12} and p_{13}. Thus, it can be inferred that the unbalanced status of v_4 and v_6 can be adjusted by balancing the power flows on the related paths: e_{12}, e_{13}, e_{24}, and e_{36}. This result indicates that the proposed control method is capable of energy management, especially power balancing and resilience.

By employing the top-down method for nodes u_0, u_1, u_2, and u_4 and the bottom-up method for node u_3, u_5, and u_6, the simulation results of the mixed control method were obtained as in Fig. 8(c), Fig. 8(f), Fig. 9(c) and Fig. 9(f). As presented in Fig. 8(c) and Fig. 9(c), the formed voltage distribution of the bottom-up side was larger than that of the top-down side, which is figured out by $v_6 > v_4$ and $v_3 > v_2$. This result indicates that power packet transmission is prioritized on the bottom-up side. Unlike the simulations of the bottom-up method or top-down method, the packet transmission between nodes 4 and 5 was regulated, *i.e.*, $p_{45} = 0$. In the path between two nodes applied with

different methods, the demand-side node requests power packets from its neighbor nodes, whereas the supply-side node does not respond to the requests with a constraint logic of the top-down algorithm, in which the "acc" message can be sent to nodes with smaller voltage than itself. As a result, the biased distributions were observed in the second stage (v_2 and v_3) and the third stage (v_4 and v_6), respectively.

The results of the above simulations indicate that a PPN is valid in the packet-based energy management and priority-based power control using the proposed control method. The proposed dynamics model applied to the decentralized algorithms, *i.e.*, consensus dynamics, the power packet transmission on a PPN follows the spread distribution. Moreover, based on the simulation with the mixed control method, the packet distribution can be adjusted according to the arrangement of nodes with the bottom-up and the top-down methods.

5. Conclusion

This paper discussed the power distribution model of a PPN and proposed a decentralized control for two operational strategies: the top-down method and bottom-up method. Based on the three-layered consensus model, we proposed a model of the agent-to-agent packet distribution of a PPN. This concept has been employed in the decentralized control for the operation of the network to follow the intended distribution model. Based on the established algorithm, we simulated the power packet transmissions on a PPN, in which the local communication was only allowed between power routers. The results indicated the structural independence of the proposed control method, as well as the novel functions for energy management, such as power broadcasting and priority-based power control. The use of the proposed control methods is expected to improve the scalability of the network topology and to solve the problem of a small-sized power system requiring delicate energy management due to the large and frequent fluctuations in the supply/demand conditions.

The proposed control method provides the possibility of advanced energy management with diverse applications; still, the system itself is low-observable. Since the control relies on agent-to-agent local interactions, an additional sensor system might be necessary to capture the changing dynamical aspects of a PPN. This is because the distribution model based on consensus dynamics only allows a qualitative analysis; thus, it cannot be directly utilized in the real-time control of a PPN. Therefore, despite the advantages, such as scalability, flexibility, and novel functions for energy management, using the proposed control methods is difficult for handling the global objective of the system, which is important in applications such as swarm robotics or multi-legged machines. Considering the possible applications of a PPN, *e.g.*, an energy distribution inspired by biomechanics, such interesting questions still remain.

Acknowledgments

This research was partially supported by Cross-ministered Strategic Innovation Promotion (SIP) Program from NEDO.

References

[1] E. Reihani, M. Motalleb, R. Ghorbani, and L.S. Saoud, "Load peak shaving and power smoothing of a distribution grid with high renewable energy penetration," *Renewable Energy*, vol. 86, pp. 1372–1379, 2016.

[2] A. Lucas and S. Chondrogiannis, "Smart grid energy storage controller for frequency regulation and peak shaving, using a vanadium redox flow battery," *International Journal of Electrical Power & Energy Systems*, vol. 80, pp. 26–36, 2016.

[3] K.M. Lynch, I.B. Schwartz, P. Yang, and R.A. Freeman, "Decentralized environmental modeling by mobile sensor networks," *IEEE transactions on robotics*, vol. 24, no. 3, pp. 710–724, 2008.

[4] J. Toyoda, "Power transactions and open electric energy network. [in Japanese]," *The Journal of The Institute of Electrical Engineers of Japan*, vol. 117, no. 6, pp. 345–348, 1997.

[5] T. Hikihara, "Power processing by Packetization and routing. [in Japanese]," *IEICE Technical Report CCS2015-57*, 2015.

[6] R. Takahashi, S. Azuma, M. Hasegawa, H. Ando, and T. Hikihara, "Power processing for advanced power distribution and control," *IEICE Trans. Commun.*, vol. E100.B, no. 6, pp. 941–947, 2016.

[7] R. Takahashi, K. Tashiro, and T. Hikihara, "Router for power packet distribution network: Design and experimental verification," *IEEE Trans. Smart Grid*, vol. 6, no. 2, pp. 618–626, 2015.

[8] R. Takahashi, S. Azuma, K. Tashiro, and T. Hikihara, "Design and experimental verification of power packet generation system for power packet dispatching system," *Proc. Amer. Control Conf.*, pp. 4368–4373, 2013.

[9] S. Nawata, A. Maki, and T. Hikihara, "Power packet transferability via symbol propagation matrix," *Proceedings of the Royal Society A*, vol. 474, no. 2213, 2018.

[10] T. Hikihara, S. Nawata, and R. Takahashi, "Power packet dispatching and dynamics in network," *Proc. 24th Int. Congr. Theor. Appl. Mech. (ICTAM 2016)*, pp. 3171–3172, 2016.

[11] E. Gelenbe and Y. Zhang, "Performance optimization with energy packets," *IEEE Systems Journal*, vol. 13, no. 4, pp. 3770–3780, 2019.

[12] E. Gelenbe, "Energy packet networks: Adaptive energy management for the cloud," *Proc. 2nd Int. Workshop Cloud Comput. Platforms*, pp. 1–5, 2012.

[13] Y. Zhou, R. Takahashi, N. Fujii, and T. Hikihara, "Power packet dispatching with second-order clock synchronization," *International Jounal of Circuit Theory and Applications*, vol. 44, no. 3, pp. 729–743, 2016.

[14] Y. Zhou, R. Takahashi, and T. Hikihara, "Security of power packet dispatching using differential chaos shift keying," *NOLTA*, vol. 7, no. 2, pp. 250–265, 2016.

[15] H. Ando, S. Azuma, and R. Takahashi, "Consensus dynamics in switching networks for distributing power packets," *The 6th IFAC Workshop on Distributed Estimation and Control in Networked Systems (NecSys2016)*, vol. 49, no. 22, pp. 351–354, 2016.

[16] H. Ando and T. Hikihara, "A bio-inspired power sharing model in consensus networks," *in Proceedings of NOLTA'18*, 2018.

[17] S. Baek, H. Ando, and T. Hikihara, "Consensus-based distributed control of power packet distribution network," *in Proceedings of JKCCS'19*, 2019.

[18] S. Baek, H. Ando, and T. Hikihara, "Consensus-based distribution of power packets and decentralized control for routing," *AIP haos: An Interdisciplinary Journal of Nonlinear Science*, vol. 30, no. 3, pp. 033115, 2020.

[19] S. Mochiyama, R. Takahashi, and T. Hikihara, "Close-loop angle control of stepper motor fed by Power packets," *IEICE Transactions on Fundamentals of Electronics, Communications and Computer Sciences*, vol. E100-A, no. 7, pp. 1571–1574, 2017.

[20] N. Fujii, R. Takahashi, and T. Hikihara, "Networked power packet dispatching system for multipath routing," *Proc. IEEE/SICE International Symposium on System Integration*, 2014.

[21] J. Michael Barrett, "Challenges and requirements for tomorrow's electrical power grid," *Future of the power grid series*, no. 2, 2016.

[22] R. Olfati-Saber, J.A. Fax, and R.M. Murray, "Consensus and cooperation in networked multiagent systems," *Proceedings of the IEEE*, vol. 95, no. 1, pp. 215–233, 2007.

[23] P. Jamieson, W. Luk, S. Wilton, and G.A. Constantinides, "An energy and power consumption analysis of FPGA routing architectures," *2009 International Conference on Field-Programmable Technology*, pp. 324–327, 2009.

[24] N. Rubido, C. Grebogi, and M. Baptista, "General analytical solutions for DC/AC circuit-network analysis," *Eur. Phys. J. Special Topics*, vol. 226, pp. 1829–1844, 2017.

[25] D.A. Spielman, "Spectral graph theory and its applications," *48th Annual IEEE Symposium on Foundations of Computer Science, IEEE*, pp. 29–38, 2007.

[26] R. Olfati-Saber and R.M. Murray, "Consensus problems in networks of agents with switching topology and time-delays," *IEEE Trans. Autom. Contr.*, vol. 49, no. 9, pp. 1520–1533, 2004.

[27] R. Riaza, "Some qualitative problems in network dynamics," *arXiv:1501.01904v1 [math.DS]*, 2015.